Motor efficiency modeling towards energy optimization for two-wheel electric vehicle

Yesid Bello, Toufik Azib, Cherif Larouci, Moussa Boukhnifer, Nassim Rizoug, Diego Patino, Fredy Ruiz

Motor efficiency modeling towards energy optimization for two-wheel electric vehicle

Article *in* Energy Efficiency · March 2022

DOI: 10.1007/s12053-021-09997-2

7 authors, including:

Cristhian Yesid Bello Ceferino
Ecole Supérieure des Techniques Aéronautiques et de Construction Automobile
4 PUBLICATIONS **6** CITATIONS
SEE PROFILE

Toufik Azib
Ecole Supérieure des Techniques Aéronautiques et de Construction Automobile
87 PUBLICATIONS **793** CITATIONS
SEE PROFILE

Cherif Larouci
Ecole Supérieure des Techniques Aéronautiques et de Construction Automobile
63 PUBLICATIONS **545** CITATIONS
SEE PROFILE

Moussa Boukhnifer
University of Lorraine
164 PUBLICATIONS **1,418** CITATIONS
SEE PROFILE

Motor Efficiency Modelling towards energy optimisation for Two Wheels Electric Vehicle.

Y. Bello, T. Azib Ph.D, C. Larouci Ph.D, , M. Boukhnifer Ph.D, N. Rizoug Ph.D, D. Patino Ph.D, F. Ruiz Ph.D.

***Abstract*— Nowadays, the transportation electrification represents one of the most significant changes to reduce the pollution production rate. Unfortunately, in a TWEV (Two Wheels Electric Vehicle), particularly in the case of a motorcycle wheel hub motor, there are different constraints by using electric driving chain. They include an autonomy reduction caused by the lack of a control system to maintain a good powertrain efficiency, principally of the motor according to the operating parameters variation. This variation is caused by the effect of the parameters like the current state of charge (SoC) of the battery, the weight of the driver, the road slope or the road/weather conditions over the motor work point. In consequence, the efficiency decreases significantly by the relationship between speed proposed by the driver and the torque required by the vehicle. Those parameters can be estimated in order to make an efficiency optimization based on present and future road/weather conditions. Regrettably, this kind of control (optimal control) requires a representative model with low computation time and easy implementation. In this paper, a convex geometrical representation of an electric motor power losses model for optimization is proposed. Its advantages over the mathematical representation are evaluated with an electric vehicle urban speed profile and an efficiency optimization compatible with the requirements of real-time operation.**

***Index Terms*— electric vehicles, longitudinal dynamic, motor efficiency, real-time, implementation**

I. Introduction

About a 56% of the total CO2 emission is related with transport field or refining processes [1], [2]. One reason of this CO2 emission can be the poor energy diversification in transport sector, about 90% of the world sector still depending of petroleum products [3]. Then, the electric vehicles represents and important factor to reduce the CO2 emission caused by transport field and in consequence, to face the greenhouse effect.

However, the energy density of power source, the efficiency of powertrain, the electric stations availability and the charge time represent some of the challenges to this technology to make it implementable. For efficiency improvements, different strategies have been proposed, in [4] the efficiency improvement opportunities in (Brushless direct current) BLDC motor are explored. In it, the external parameters and the work point represent the main tool to develop efficiency optimizations. As another example, in [5], the optimization of downhill speed/torque parameters are achieved to maximize the efficiency of regenerative brakes with hydraulic brakes coolaboration. This approach lets to note the efficiency of the motor can be optimized taking into account the external parameters. In the same way and in order to improve the efficiency of powertrain specifically, this paper proposes the study of urban mission profile effect over the power losses as a tool to describe the requirements of an optimal mission profile (an eco-driving profile). Optimal mission profile will be able to propose speed limitations based in torque, temperature behavior in order to keep the maximum efficiency of power train. The dyanmic model is the most important aspect to be considered in order to propose an optimization to maximize the performance and availability of electric vehicles according to the urban requirements [6]. In electric powertrain, the modelization has to cover mainly two aspects: The electrical and the mechanical behavior. The electrical diagram of the vehicle usage is shown in Figure 1, where Vx_r, Idq_r, Vdq, Udc, Cr, $Iabc$, Idq, C, Ω are the longitudinal reference speed, direct and quadrature reference currents, direct and quadrature reference voltages, DC voltage, the load torque, the motor phases currents, the direct and quadrature currents measured on the motor, torque measured on the motor and the angular speed measured on the motor.

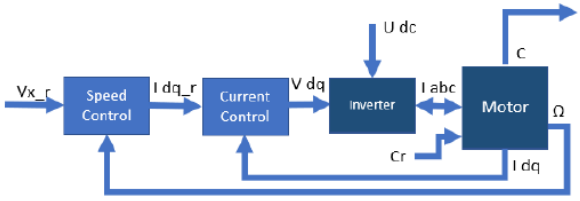

Fig. 1: General control diagram of a BLDC motor.

The most important aspect related to energy optimization are the energy losses in each component of the electric powertrain due to the driver behavior [7]. If just electrical losses are considered, the main three sources of power losses are the battery, the driver and the motor. Then, it is possible to create constraints over the driver behavior keeping in mind the motor remains the most affected by efficiency variation [8]. In this paper, the losses caused in the motor will be studied and modeled in order to obtain an appropriate efficiency behavior to be integrated into the optimization

Y. Bello(*), A. Patino, and F. Ruiz : are with the Department of Electronics Engineering, Pontificia Universidad Javeriana, Bogot, D.C. , Colombia. (*corresponding author; e-mail: cristhian.bello@javeriana.edu.co). T. Azib, C. Larouci, M. Boukhnifer, N. Rizoug are with the Energy and Embedded Systems for Transportation Research Department, ESTACALAB, Montigny-Le-Bretonneux, France.

process. The complexity of this kind of model difficult real-time optimization. For this reason, new compile time efficient approaches are required.
This paper will be developed as follows: In the second section, the motor losses in an electric motor will be classified to be studied and the hypothesis required by calculus will be shown. In the third section, the analytical model of the motor will be developed. The fourth section will present the efficiency map developed according to the considered requirements. The fifth section presents the geometrical representation of the efficiency map obtained before and the constraints required to represent the efficiency with the minimum error. In section sixth, the error obtained by the geometrical representation will be analyzed to determine the usability of the geometrical representation in the optimization process. Finally, conclusion and future work will be proposed.

II. Electric Motor power losses.

The electric motor highlight by its efficiency in comparison with other kinds of engines available in the transport field. Although there are many methods to estimate or measure the load motor efficiency under the full speed condition, few of them are capable to estimate the efficiency under variable speed conditions. For this reason, variable speed/load efficiency models are required. Since the transport field represents a variable load and speed references, the motors efficiency tends to decrease dramatically. In [9], a data-based model is proposed to estimate the efficiency face on speed changes. The model estimates an equation capable to describe the core, friction and copper losses behavior from measured data. This method is able to reduce significantly the error in low speed/torque region but it is not able to explain the causes of the behavior of each source of energy loss. In order to make a complete analysis, each kind of energy loss will be discused and represented by an analytical equation.
The most evident losses source is power dissipation (Joule Losses). In [10] it is explored in order to ensure an improvement over the efficiency estimation. Indeed, the efficiency of the inverter and the motor are calculated ensemble to compare the theoretical developments with measures made in different work points. Even when this approach is able to reproduce the efficiency behavior with less than a 10% of error (this value grow up linearly with the speed value), it has a disadvantage, it is blind in face of other energy losses sources, it can be noticed due to the non constant behavior of the error.
In another study [11], a model based on the machine equivalent circuit is presented. This model is capable to use the no-load and full-load test to reproduce four kind of losses : Cooper losses, Core losses due to hysteresis and Eddy current, viscous friction losses and joule losses present in stator and inverter. The accuracy of this approach is comparable to the 10% described in the first paper but its error does not grow up with the speed of torque. In other words, even when the accuracy of the method has to be improved, it is capable to represent most of the power losses sources.
The approach exposed before mixed the inverter and motor losses. It makes difficult to make optimizations over the motor structure or the motor energy requirements. Then, another approach is explored in [12], [13] and [14]. The joule, core and copper losses caused inside the motor are analysed througth making an electromagnetic analysis. In [14], Steinmetz and Bertotti equations are compared to determine that Bertotti equation is capable to make a better representation of the stator core losses in flux weakening region due to it has into account the dynamic of the magnetic flux density. The magnetic flux density is a variable which is difficult to represent in time then, the effect of its harmonics is studied theoretically [15] and after, it can be compared with two software applications or direct measures over the motor. The first software application is a representation of the magnetic flux density as a function of the current present in the stator through finite-element analysis (FEA) [16], [17]. This representation requires three lookup tables, the magnetic flux density as a function of stator current measured in the stator yoke, the rotor yoke, and the air gap. In [14], the representation of the magnetic flux density in the stator is separated in the magnetic flux density present in the body of the tooth and the tooth tip. This differentiation lets to reduce the average error of the algorithm. Some examples of software used to represent the magnetic flux density are ANSYS/Maxwell, Altair/Flux2D and COMSOL. The second software appication is a direct representation of the efficiency map made by a logical programming working ensemble of the magnetic simulation software, this option is available few software like ANSYS/Maxwell. However, this option also requires a comprehension of the theoretical model, it lets to know which kind of excitation is required to represent the different power losses.
Last of the most important parameters to consider in motor efficiency is the temperature effect. In order to model the thermal behavior, a thermal circuit has to be considered. It will consider a few quantities of thermal nodes if just the effect of temperature over losses wants to be considered [18] or a huge quantity if design aspects want to be evaluated. When many thermal nodes want to be considered, the FEA study is required [19]. This study consider a in-wheel motor of medium power, for this reason, the passive air cooling system use to be enough to control temperature risks.
In conclusion, the power sources from the motor have to be studied separated to the inverter or battery power losses sources and the phenomenon represented will be:

- Copper losses, it is called Joule losses too and it makes reference to the power dissipation due to the current trajectory along the copper wires in the stator.
- Core losses, It represents the power losses in stator and rotor due to Eddy currents and Hysteresis effect.

Also, the power losses calculation will be made under the following assumptions:

- The input current is assumed to be ideal sinusoidal.
- The effect of the inverter and power source losses is well ignored through simulation.

- The passive cooling system effectivity is as high to not consider the temperature effect over each operation point (speed/Torque).
- Mechanical friction loss effect can be ignored.
- The effect of the magnetic flux density dynamic is minimum due to the size of the air gap and the stator/rotor materials properties.

III. Power losses Model.

The BLDC Motor model can be described by the following equations using d-q analysis:

$$\begin{aligned} U_d &= \frac{d\Psi_d}{dt} - \Psi_q W_s + R_s i_d \\ U_q &= \frac{d\Psi_q}{dt} + \Psi_d W_s + R_s i_q \end{aligned} \tag{1}$$

where U_d, U_q, i_d and i_q are the d-and q-axis stator voltages and currents. R_s, W_s, R_s, are the stator resistance, the electrical angular speed that equals the multiplication of the rotor mechanical speed and the number of pole pairs p; Finally, Ψ_d and Ψ_q are the d-and q-axis stator fluxes which are equal to:

$$\begin{aligned} \Psi_d &= L_s i_d + \Psi_r \\ \Psi_q &= L_s i_q \end{aligned} \tag{2}$$

Where L_s represents the stator inductance and Ψ_r represents the permanent magnet flux. Then the electromagnetic torque generated is:

$$T_e = \frac{2}{3} p(i_q \Psi_d - i_d \Psi_q) \tag{3}$$

The permament magnets lets to make flux control throw the the direct-axis current minimization the magnetisation and the quadrature-axis current maximization in order to incremet the quantity of energy used in torque production and reduce the "current waste". When i_d tends to "0", the expression changes as follow:

$$T_e = \frac{2}{3} p(i_q \Psi_d) \tag{4}$$

The mechanical equation is:

$$\frac{J}{p}\frac{dW_s}{dt} = T_e - T_l \tag{5}$$

Where J, W_s, T_l are the moment of inertia of the rotor, the mechanical angular speed of the rotor, and the load torque. Since efficiency in stady state can be defined as:

$$\eta = \frac{P_{out}}{P_i} = \frac{T_e W_s}{T_e W_s + P_{lcu} + P_{lfe} + P_{lmag}} \tag{6}$$

Where, P_{lcu}, P_{lfe} and P_{lmag} are the Joule losses (also called iron losses), the core losses and the magnetic losses in rotor magnets.

A. Magnetic Losses

The magnetic losses caused by eddy-current loss in the permanent magnets of brushless machines are usually neglected. Since the fundamental air-gap field usually rotates in synchronism with the rotor, and time harmonics in the current waveform in the winding distribution are generally small [12]. For this reason, $P_{lmag} \approx 0$.

B. Joule losses

The joule losses can be estimated according to following approach [20], [13]:

$$P_{lcu} = \frac{\frac{\rho_{cu}}{K_{fill}}(L + L_{ew})(K_{sp}\pi D_o)}{\frac{\pi}{4}(D_o^2 - (D_i + \frac{B_g \pi D_o}{B_j 2pK_{fe}})^2) - \frac{B_g \pi D_o}{B_t}(\frac{D_o - D_i}{2} - \frac{B_g \pi D_o}{4B_j pK_{fe}})} \tag{7}$$

Where ρ_{cu}, D_o, D_i, B_g, B_t, B_j, K_{fill}, F_{fe}, p, L, L_{ew}, K_w and K_{sp} are the copper resistivity [Ohm.m], the stator outer diameter [m], the stator inner diameter [m], the air gap flux density [T], the flux density in stator tooth [T], the flux density in stator yoke [T], the slot filling factor, the lamination factor, the number of pole pairs, the stator lamination length [m], the length of end-winding [m], the fundamental winding factor, and the fundamental current density [A/m], which can be expresed in terms of load torque "T_l".

$$K_{sp} = \frac{T_l}{B_g D_o^2 L sin(p\alpha_{pm})} \tag{8}$$

where α_{pm} is the half of mechanical magnet angle.

C. Core Losses

The core losses are composed of losses caused by hysteresis losses and eddy current losses. By one hand, the hysteresis losses are the resistance of a magnetic material to change its magnetic field orientation. By the other hand, the eddy current losses are the undesired current provoked by magnetic fields. Those current are strongly related to winding architecture, for this reason, the minimization of the eddy current losses harmonics can be made studying and optimizing the winding structure [21].
The core losses under any operating condition can be estimated as follows [14].

$$P_{lfe} = P_{l_e dd_y oke} + P_{l_t} + P_{l_{tt}} \tag{9}$$

Where, $P_{l_e dd_y oke}$, P_{l_t} and $P_{l_{tt}}$ are the losses in rotor yoke due to eddy current and losses in tooth body and tooth tip caused by hysteresis and eddy current.

Those expresion are:

$$P_{l_e dd_y oke} = n_y (\frac{f}{p})^{1.5} R^2_{y_m ean} A_{ry} \sqrt{\frac{\pi^2}{i \rho_{Fe} \mu_{Fe}}} \sum_{i=1}^{\inf} \frac{B_i}{\sqrt{i}} \tag{10}$$

$$P_{l_t} = K_h f^{\alpha} B_t^{\beta} + \frac{4}{\pi} K_e \frac{f^2 B_t^2}{\alpha_t} \tag{11}$$

$$P_{l_{tt}} K_h f^{\alpha} B_{tt}^{\beta} + \frac{4}{\pi} K_e \frac{f^2 B_{tt}^2}{\alpha_{tt}} \tag{12}$$

Where n_y, f, p, R_{y_mean}, A_{ry} are the number of rotor yokes, frequency, number of poles pairs, mean radius of the rotor yoke, tha area of the rotor yoke face. ρ_{Fe}, μ_{Fe}, B_i, B_{tott} and α_{tott} are resistivity and the mean permeability of the rotor yoke material, the magnitude of ith harmonic of the armature flux density wave, the peak value of flux density at the tooth or the tooth tip and the mean pole transition angle in electrical radians. Finally K_h, α, β and K_e are constants obtained from the curve fitting of core loss data measured with sinusoidal excitation. Since it was mentioned in section II, this representation requires three lookup tables, the magnetic flux density as a function of stator current measured in the stator yoke, the rotor yoke, and the air gap. In this paper, all those expressions are introduced by two reasons:

- Defend some hipothesis in following sections.
- Determine the correct excitation parameters in the direct representation of the efficiency map made by a magnetic simulation software.

IV. Results.

A. Efficiency Map

The efficiency map was obtained from a direct representation made by a logical programming working ensemble with a magnetic simulation software. The parameters of the electric motor evaluated are:

Parameter	Value
The rated voltage	72 v
The rated power output	3000 w
The rated torque	185.6 Nm
The rated speed	91.3 RPM
No Load maximum speed	157.6 RPM
Maximum efficiency speed	773 RPM
Maximum efficiency torque	73.2 RPM
Maximum efficiency	96.4 %
Pole pairs	16
Outer diameter of the motor	253.3 mm
Magnet Height	50 mm
Number of turns per coil	30
Phase resistance	0.03 Ω
Phase inductance	0.04 mH

TABLE I: Motor parameters

Also, the excitations required to study the core and the copper losses are:

- Winding (current). It is the current for both, a stranded and solid conductor. This excitation lets to represent the eddy current and hysteresis effect caused by an AC signal.
- Current. It represents the total current in a conductor. This excitation lets to represent the joule losses.
- Coil. Used to define one or more model winding. It is required as a model component but it will determine the copper and core losses behavior too.

Finally, the efficiency map obtained is:

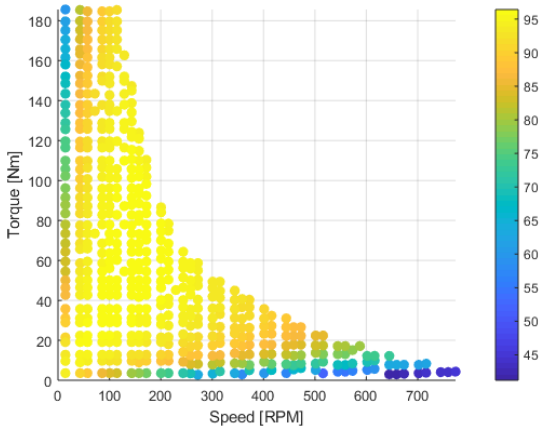

Fig. 2: Efficiency map obtained by electromagnetic simulation software.

B. Geometric representation of the efficiency map

The objective is to replace the mathematical equation which describes the efficiency by a convex surface able to be used as an optimization surface. For this reason, after analysing the efficiency map data behavior, an elliptic paraboloid is used to describe the efficiency. The general equation of the hyperboloid is:

$$Z = B_0 - \frac{X^2}{a^2} - \frac{Y^2}{b^2} \tag{13}$$

Where X, Y, Z represent the efficiency, the torque and the speed. Equation 13 describes an elliptic paraboloid with center in $(0, 0, B_0)$. Also the values a and b will describe the elliptical curves on each Z value. In other words, the values a, b will describe the slope in the axis X and Y respectively. In order to use a linear regression over the data the equation is reorganized like this:

$$Z = B_0 - B_1 X_s - B_2 Y_s \tag{14}$$

Where:

$$\begin{aligned} B_1 &= \tfrac{1}{a^2} \\ B_2 &= \tfrac{1}{b^2} \end{aligned} \tag{15}$$

and

$$\begin{aligned} X_s &= (X - x_c)^2 \\ Y_s &= (Y - y_c)^2 \end{aligned} \tag{16}$$

After the linear regression is made, the B coefficients and

the centroid of the paraboloid are:

Parameter	Value
B_0	95.79
B_1	1.3149e-4
B_2	0.0013
x_c	157.65
y_c	73.2

TABLE II: Paraboloid parameters.

A comparison between the paraboloid surface and the efficiency map data is shown in Figure 3:

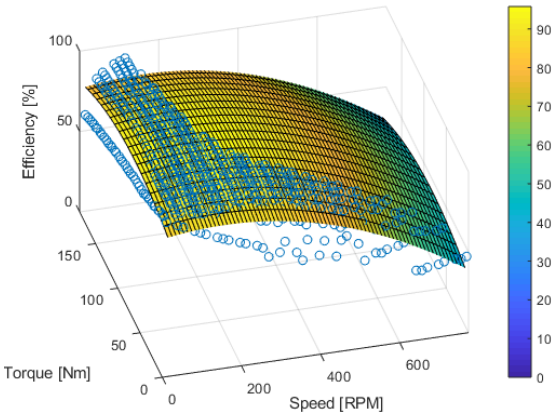

Fig. 3: Hyperboloid representation of the efficiency map.

The surface resultant is available from a range from 0 Nm to 185Nm and from 0 RPM to 800RPM. But in the efficiency map, it exists a curve which divided the feasible region from the non-feasible region. It is called the maximum power curve. If the core and iron motor losses are not taken into account, the maximum power curve can be expressed as:

$$T_{Lim} = \frac{P_{max} * \eta_{bat} * \eta_{inv} * \eta_{mot}}{RPM * R_w * 0.10472}; \qquad (17)$$

Where $P_{rated}, \eta_{bat}, \eta_{inv}, \eta_{mot}, RPM, R_w$ are the rated power, the average battery efficiency, the average inverter efficiency, the average motor efficiency caused by Joule losses, the speed in RPM and the wheel radius. Unfortunately, In Figure 4, the effect described in [10], by ignoring core and iron losses can be appreciated (An error which increases with the speed value). In order to keep the model simple, a set of four lines are made to represent the speed limit based on the torque value.
Now that both surfaces have the same limitations, they can be compared to evaluate the error from the geometrical representation in comparison to the efficiency map data.

V. Error Analysis

Even when the mean percentage error is about 0% and the mean absolute percentage error is 4.04% along all the surface, there are two regions where the surface presents an error over the 5%. Those regions are placed close to the origin of the torque and speed axis and they represent the minimum efficiency values. It is important to notice that the geometrical representation has its minimum values in the same region but the values are not the same than the efficiency map.
The effect of the error between the efficiency map data and the geometrical representation obtained has to be evaluated under three situation: Along all the possibles values, under a urban driving cycle and under an optimized drive cycle. In order to use the geometrical representation of the efficiency map, the power limitation has to be expressed.

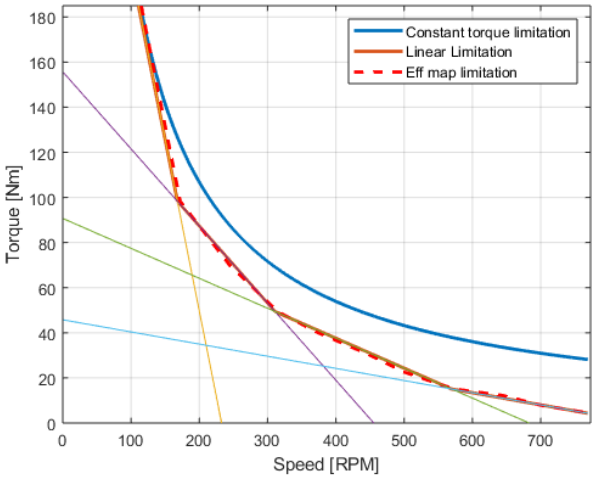

Fig. 4: Power limitation over geometrical representation.

A. Along all the possibles values

As it was mentioned before, the average error is about 0 along all the surface but the average of the absolute error is 4.04% (Figure 5). It means that if the motor would be able to recreate the efficiency data with the same range, the positive and negative error in the measures would be canceled. But in the real drive cycle there are speed limitations imposed by the traffic zones and also, by the electric devices required to make the motor move. This is why a more complete study is required.

B. Along an urban drive cycle

In order to obtain a torque and speed profile able to be used as the reference to this research, the NREL Classe 6 drive cycle developed by Smith Newton from NREL Labs [22] was used. This driving profile was designed for electric vehicles in an urban environment. The speed profile requires a characterization of the electric vehicle and the road characteristics to obtain the torque profile. The electric vehicle characteristics are shown in Table III.

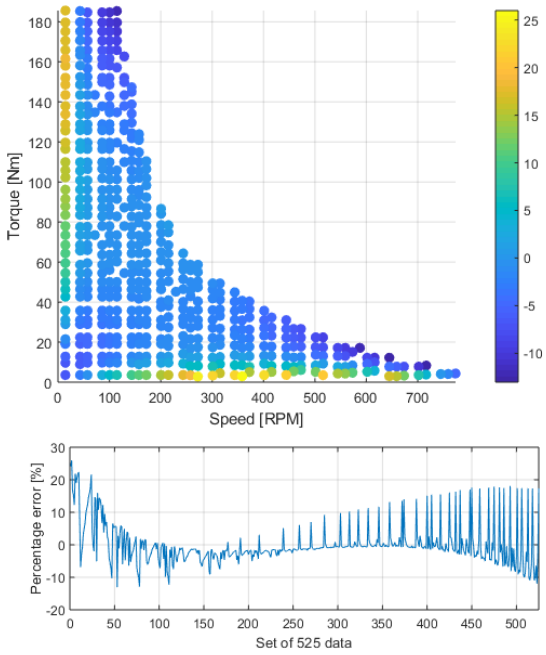

Fig. 5: Error of geometrical representation.

Parameter	Value
M	150.00 [Kg]
A_f	0.94 [s^2]
Rwr	0.58 [m]
ρ	0.96 [$\frac{Kg}{m^3}$]
C_d	0.40
g	9.81 [$\frac{m}{s^2}$]

TABLE III: Vehicle and environment characteristics.

Finally, the slope trajectory was taken from a trip from Paris to Brussels. The longitudinal force modelation used to obtain the torque profile is based on Newtons second law of motion along the X axis.
According to [23], [24] and [25], the most relevant negative forces related to energy losses are:

- Aerodynamic force.
- Rolling resistance force.
- Slope of the road.

Then, the Longitudinal dynamic is described as:

$$M(\ddot{x}) = \frac{T_f}{R_{wf}} + F_{roll} + F_{aer_x} + F_w sin(\theta_s) sin(\beta) \quad (18)$$

Where $R_{wf}, F_{roll}, F_{aer_x}, F_{w,s}, \beta$ are the effective radius of rear wheel, roll resistance, aerodynamic force associated to X-axis, weight, slope angle and bank angle.

a) Aerodynamic force: It can be expressed as:

$$F_{aer_x} = \frac{-1}{2} \rho C_d A_f V_x^2 \quad (19)$$

Where $\rho, C_d, A_f, \dot{x}, V_x$ are the air density, drag coefficient, front area and longitudinal vehicle speed.

b) Rolling Resistance Force: It can be expressed as:

$$F_{roll} = -(\mu_0 + \mu_1 \dot{x}^2) F_z cos(\theta_s) \quad (20)$$

Where μ_0, μ_1 are two friction coefficients of the road, F_z is the normal force of the vehicle and θ_s is the slope of the road. The friction coefficients of the road depend on the state of the road. For example, a new asphalt is [0.01, 0.008] and the frozen asphalt is [0.001, 0.00082].

c) Slope of the road: When the road presents a slope by a medium or long distance, the load exchange cannot be ignored. In this case, the load exchange has not a dynamic but it creates a weight component in X and Y axis which affects the forward and lateral movement dynamic. The equation which describes this effect is:

$$F_w = mg \quad (21)$$

Where m, g the mass and gravity.
As a result of the speed follow made with data presented, the torque profile show in Figure 6.

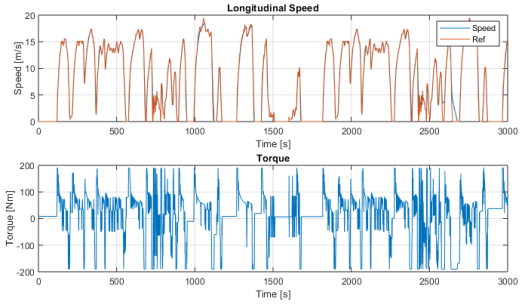

Fig. 6: Urban profile.

In Figure 7, the value of efficiency of each torque-speed couple is shown. The profile is able to cover the most of the surface superface except by the spped limitation of 30 $\frac{m}{s}$ imposed by the motor driver to protect the battery and the motor.
The average error is 0.88% allong the trajectory (30 000 samples) but the average of the absolute error increases to 3.73%. The minimum error efficiency value was -6.87% and the maximum was 24.19% when the speed is close to cero but the road requires high values of torque to achieve this low speed. In conclusion, the geometrical representation of the efficiency map is able to reproduce the efficicency with an average absolute error of 3.73%, which is acceptable considering the simplicity of the model in comparison with the theoretical model presented in Seccion III.

C. Along an optimized drive cycle

In order to determine how the error of the geometric representation of the efficiency map affects an optimized drive cycle, the following optimization was made:

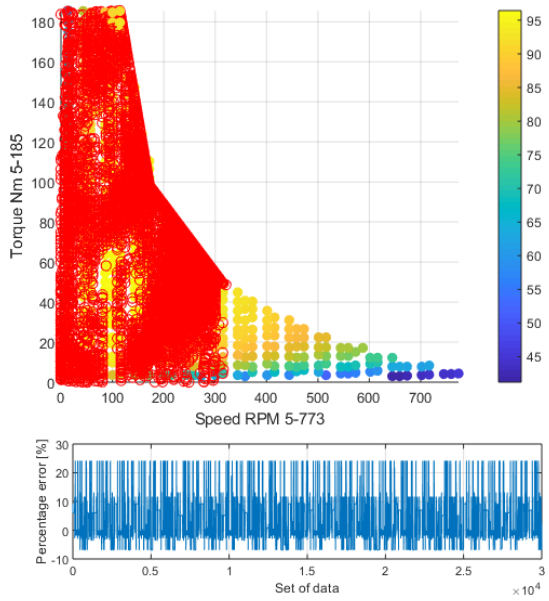

Fig. 7: Error of efficiency along a urban profile.

$$
\begin{aligned}
&minJ(x)\\
&J(x) = -Z = -B_0 + B_1X_s + B_2Y_s\\
&s.t.\\
&-T_{max} \leq U \leq T_{max}\\
&0 \leq x_2 \leq V_{max}\\
&\dot{x} = f(x,u)
\end{aligned}
\tag{22}
$$

where $\dot{x} = f(x,u)$ is represented by (18).

a) Cost Function: The goal is to minimize the energy required to complete a trip then, the cost function represents the maximization of the efficiency function without takes into account any traffic limitation, just the speed limitation imposed by the inverter.

b) State and control constraints: The state constraints were obtained from a QSMOTOR of 3000W [26]. Those constraints are:

Parameter	Value
T_{max}	185 [Nm]
V_{max}	30 $[\frac{m}{s}]$

TABLE IV: State constraints.

As a result of the speed optimization based on the torque demand by the external parameters, the torque profile shown in 8 is obtained. This driving profile does not consider the external obstacles like traffic ligth, other vehicle or curves, but it lets to calculate what is the effect of the error between the geometric representation of the efficiency map and the efficiency map when an optimized speed profile is followed. Since it is shown in 9, the efficiency value along all the trip is close to the paraboloid centroid. the average error is -2.21% along the trajectory (30 000 samples), in this case, the average of the absolute error does not increase too much (2.26%). The minimum error efficiency value was -7.49% and the maximum was 21.65% when the speed is close to zero. In conclusion, the geometrical representation of the efficiency map is able to reproduce the efficiency with an average absolute error of 2.26%, in the optimized conditions. This value is better than the 3.73% when an urban driving profile is applied and the difference between them is enough small to conclude that the geometrical representation of the surface is an acceptable approximation of the theoretical efficiency function in both cases.

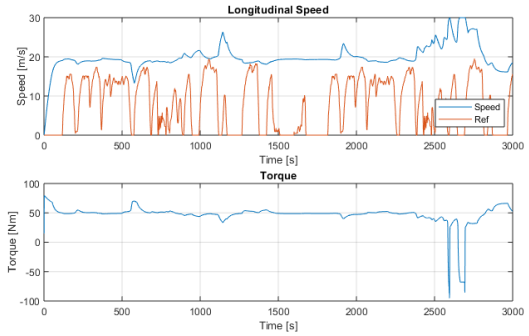

Fig. 8: Optimizated profile.

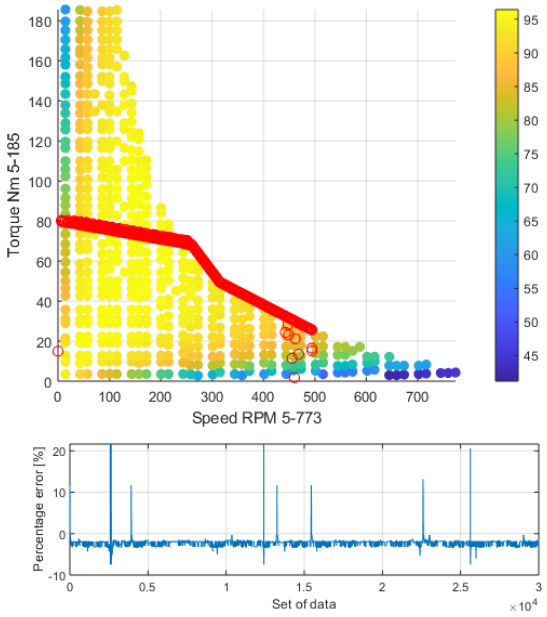

Fig. 9: Error of efficiency along an optimizated profile.

Besides, the compilation time required to make an speed profile optimization was reduced a 80.22% in comparison with a cost function which uses an efficiency equation proposed by [27].
The equation is:

$$
\eta = \frac{1}{1 + \frac{R_s}{3/2p\Psi^2}\frac{T}{\Omega} + \frac{L_s^2}{R_s}\frac{T\Omega}{3/2p\Psi^2}} \tag{23}
$$

Where, $\eta, R_s, p, \Psi, T, \Omega, L_s$ are the efficiency, the stator resistance, the number of pole pairs, the permanent magnet

flux, the mechanical torque, the mechanical speed and the stator inductance. This equation under estimes the friction, iron and core loss.

VI. Conclusion and Future Work

In this paper, a geometric representation of a complex electromagnetic model of a BLDC Motor efficiency was developed. The effect of the error of the geometrical representation obtained was evaluated under three situation: along all the possibles values, under an urban driving cycle, and under an optimized drive cycle. In all cases, the geometrical representation was able to obtain an average absolute error under the 4.1%, this value decreases when an urban driving profile is applied with the speed constraints caused by the inverter and the traffic to 3.73% and it decreases even more (2.26%) when an optimized driving profile is applied. As a conclusion, the geometrical representation of the efficiency map is acceptable considering the simplicity of the model in comparison with the complete theoretical model and it is able to reduce significativily (about an 80%) the compilation time in comparison with other efficiency model proposed.
In future works, the theoretical model requires to consider the temperature effect and the variation of the electric brakes energy harvest capacity. Besides, the mission profile optimization has to be constrained with more realistic traffic requirements. In order to keep high energy saves, new degrees of freedom over the energy direction, brake system, and energy sources need to be added.

References

[1] R. Iv, A. Zeki, and . Mohovi, "Comparison of CO 2 Emissions for Road and Sea Transport on the Specific Route," in *60th International Symposium ELMAR-2018*, no. September, pp. 16–19, 2018.

[2] P. Li, P. Zhao, and C. Brand, "Future energy use and CO 2 emissions of urban passenger transport in China : A travel behavior and urban form based approach," *Applied Energy*, vol. 211, no. November 2017, pp. 820–842, 2018.

[3] S. Gota, C. Huizenga, K. Peet, N. Medimorec, and S. Bakker, "Decarbonising transport to achieve Paris Agreement targets," *Energy Efficiency*, pp. 363–386, 2019.

[4] N. Shah, N. Sathaye, A. Phadke, and V. Letschert, "Efficiency improvement opportunities for ceiling fans," pp. 37–50, 2015.

[5] L. Li, X. Li, X. Wang, J. Song, K. He, and C. Li, "Analysis of downshift ' s improvement to energy efficiency of an electric vehicle during regenerative braking," *Applied Energy*, vol. 176, pp. 125–137, 2016.

[6] X. Zhou, D. Qin, and J. Hu, "Multi-objective optimization design and performance evaluation for plug-in hybrid electric vehicle powertrains," *Applied Energy*, vol. 208, no. 174, pp. 1608–1625, 2017.

[7] J. C. Ferreira, V. Monteiro, and J. L. Afonso, "Dynamic range prediction for an electric vehicle," *2013 World Electric Vehicle Symposium and Exhibition, EVS 2014*, pp. 1–11, 2014.

[8] C. Yang, S. Du, L. Li, S. You, Y. Yang, and Y. Zhao, "Adaptive real-time optimal energy management strategy based on equivalent factors optimization for plug-in hybrid electric vehicle," *Applied Energy*, vol. 203, pp. 883–896, 2017.

[9] Y. Li, M. Liu, J. Lau, and B. Zhang, "A novel method to determine the motor efficiency under variable speed operations and partial load conditions," *Applied Energy*, vol. 144, pp. 234–240, 2015.

[10] M. Markovic, A. Hodder, and Y. Perriard, "An analytical determination of the torque-speed and efficiency-speed characteristics of a BLDC motor," *2009 IEEE Energy Conversion Congress and Exposition, ECCE 2009*, vol. 6, no. 5, pp. 168–172, 2009.

[11] T. Ishikawa, T. Tsuji, S. Hashimoto, and N. Kurita, "Simple Equivalent Circuit for Efficiency Calculation of Brushless DC Motors," *Journal of international Conference on Electrical Machines and Systems*, vol. 3, no. 1, pp. 54–60, 2014.

[12] T. Toma, "Rotor Loss in Permanent-Magnet Brushless AC Machines," *Genome Biology*, vol. 2, no. 1, pp. 1612–1618, 2001.

[13] C. Li, H. Zhu, M. Wu, and Z. Jiang, "Efficiency Map Calculation for Surface-mounted Permanent-magnet In-wheel Motor Based on Design Parameters and Control Strategy," *Jianzhu Cailiao Xuebao/Journal of Building Materials*, vol. 19, no. 6, pp. 1–6, 2016.

[14] M. Fasil, N. Mijatovic, B. B. Jensen, and J. Holboll, "Nonlinear Dynamic Model of PMBLDC Motor Considering Core Losses," *IEEE Transactions on Industrial Electronics*, vol. 64, no. 12, pp. 9282–9290, 2017.

[15] Z. Tian, C. Zhang, and S. Zhang, "Analytical calculation of magnetic field distribution and stator iron losses for surface-mounted permanent magnet synchronous machines," *Energies*, vol. 10, no. 3, 2017.

[16] P. Dusane, "Simulation of BLDC Hub Motor in ANSYS - Czech Technical University in Prague Faculty of Electrical Engineering Department of Power Engineering Student : Prathamesh Mukund Dusane," no. June, 2016.

[17] H. M. Cheshmehbeigi and E. Afjei, "Design Optimization of a Homopolar Salient-Pole Brushless DC Machine : Analysis , Simulation , and Experimental Tests," *IEEE Transactions on Energy Conversion*, vol. 28, no. 2, pp. 289–297, 2013.

[18] P. Ragot, S. Member, M. Markovic, Y. Perriard, S. Member, and A. Overall, "Optimization of Electric Motor for a Solar Airplane Application," vol. 42, no. 4, pp. 1053–1061, 2006.

[19] S. Nategh, S. Member, O. Wallmark, and M. Leksell, "Thermal Analysis of a PMaSRM Using Partial FEA and Lumped Parameter Modeling," *IEEE Transactions on Energy Conversion*, vol. 27, no. 2, pp. 477–488, 2012.

[20] N. Bianchi, S. Bolognani, and P. Frare, "Design criteria of high efficiency SPM synchronous motors," *IEMDC 2003 - IEEE International Electric Machines and Drives Conference*, vol. 2, pp. 1042–1048, 2003.

[21] Z. Zhang, Z. Deng, C. Gu, Q. Sun, C. Peng, and G. Pang, "Reduction of Rotor Harmonic Eddy-Current Loss of High-Speed PM BLDC Motors by Using a Split-Phase Winding Method," *IEEE Transactions on Energy Conversion*, vol. PP, no. c, p. 1, 2019.

[22] R. Prohaska, A. Duran, A. Ragatz, and K. Kelly, "Statistical Characterization of Medium-Duty Electric Vehicle Drive Cycles," in *The 28th International Electric Vehicle Symposium and Exhibition*, no. May, 2015.

[23] R. N. Jazar, *Vehicle dynamics*. Springer, 2014.

[24] Z. Younes, L. Boudet, F. Suard, M. Gerard, and R. Rioux, "Analysis of the main factors influencing the energy consumption of electric vehicles," *2013 International Electric Machines & Drives Conference*, pp. 247–253, 2013.

[25] P. Fajri, V. Anand, K. Prabhala, and S. Member, "Emulating On-Road Operating Conditions for Electric-Drive Propulsion Systems," *IEEE Transactions on Energy Conversion*, vol. 31, no. 1, pp. 1–11, 2016.

[26] QSMOTOR, "Torque Test," 2017.

[27] C. M. Xi Zhang, *Vehicle Power Mangement*. Springer, i ed., 2011.